Genesis of the periodic lattice distortions in the charge density wave state of 2H-TaSe_{2}

Valeri Petkov, Kamal Chapagain, Sarvjit Shastri, and Yang Ren

Phys. Rev. B **101**, 121114 — Published 19 March 2020

DOI: 10.1103/PhysRevB.101.121114

Genesis of the Periodic Lattice Distortions in the Charge-Density-Wave State of *2H*-$TaSe_2$

Valeri Petkov,[1,*] Kamal Chapagain,[1] Sarvjit Shastri,[2] and Yang Ren[2]

[1]*Department of Physics, Central Michigan University, Mt. Pleasant, Michigan, 48858, USA*

[2]*X-ray Science Division, Advanced Photon Source, Argonne National Laboratory, Argonne, Illinois, 60439, USA*

(Received; published)

Using high-energy x-ray diffraction and large-scale 3D structure modeling, we reveal the evolution of local lattice distortions in the archetypal charge density wave (CDW) system *2H*-$TaSe_2$ as it is cooled from its normal state above room temperature down to temperature where Ta atoms form a long-range ordered superstructure. In particular, we find that the structure is formed via a gradual in-plane clustering of Ta atoms exhibiting unusually short bonding distances already near room temperature, and not via a cooperative distortion of Ta atomic planes taking place at the critical ordering temperature. Our findings clarify the debated local symmetry and magnitude of the periodic lattice distortions in the CDW state of *2H*-$TaSe_2$, and emphasize the role of locally correlated lattice distortions as a precursor of CDWs in low dimensional solids. Also, we demonstrate an efficient experimental approach to study them.

DOI:

Charge density waves (CDW)s in low-dimensional solids are a subject of extensive research due to their relevance to fascinating quantum phenomena such as superconductivity. Also, they hold promise for practical applications in the fields of ultrafast electronics and optics. Currently, the CDW state is understood as a long-rage modulation of the electron density coupled to a periodic distortion of the crystal lattice (PLD) emerging below a critical ordering temperature, T_{CDW} [1-7]. While PLDs in the regime both of weak and strong coupling CDWs are well studied, little is known about the nature of lattice distortions above T_{CDW}, and their relationship to the PLDs below T_{CDW}. This is because lattice distortions related to CDWs are largely studied by imaging and crystallographic techniques that are difficult to apply when the distortions are less-well defined or not perfectly periodic, as they usually are above T_{CDW} [8-11]. Here we use experimental techniques that are applicable to systems with any degree of structural distortions and periodicity to study the evolution of lattice distortions in the archetypal CDW system 2H-$TaSe_2$ over a broad temperature range. We find that lattice distortions in this system appear as unusually short Ta-Ta bonding distances already near room temperature. The distances fluctuate due to thermal excitations but become increasingly correlated locally with decreasing temperature, reflecting the formation of small clusters of Ta atoms characteristic to the CDW/PLD state of 2H-$TaSe_2$ well before it emerges. The clusters are well-separated from each other above T_{CDW} and merely form a superstructure when T_{CDW} is reached. Our observation of persistent Ta clustering above T_{CDW} indicates that the long-range ordered CDW/PLD state in 2H-$TaSe_2$ emerges via a gradual buildup of locally correlated lattice distortions, and not via a spontaneous emerging of uniform lattice distortions at T_{CDW}. The finding sheds new light on the genesis of CDW/PLDs in low-dimensional solids and prompts for further investigations.

The compound 2H-$TaSe_2$ belongs to the widely studied family of transition metal chalcogenides, which, depending on the chemical composition, parent structure type and temperature, appear in various CDW/PLD states [1, 12-14]. At an atomic level, 2H-$TaSe_2$ may be looked at as a stack of Ta-Se layers held together by weak wan der Waals interactions. In a layer, Ta atomic plane is sandwiched between two hexagonal Se atomic planes, forming strong ionic bonds within a local trigonal prismatic unit (FIG. 1f). In the high temperature normal state, 2H-$TaSe_2$ is a bad metal with pseudogap and c-axis resistivity 20-50 times larger than the in-plane resistivity. It undergoes a transition to an incommensurate (I) CDW/PLD phase at $T_{(I)CDW}$ ~ 122 K with a modulation close to a $3a \times 3a$ superstructure followed by another transition into a commensurate (C) $3a$ x $3a$ CDW/PLD phase at $T_{(C)CDW}$ ~ 90 K, where a is the plane lattice parameter. Concurrently, a CDW energy gap of approximately 80 meV appears [1, 15-19]. In the CDW/PLD state of 2H-$TaSe_2$, Ta atoms appear displaced from their position in the undistorted hexagonal lattice forming a repetitive pattern of small planar clusters. The in-plane static displacement of Ta atoms has been found to be much larger than that of Se atoms [20-26]. To date, no well-defined lattice distortions have been identified above the temperature of the onset of the first (I)-CDW/PLD phase. However, observed "pseudogap"-like features, strong two-phonon mode in Raman spectra and significant diffuse x-ray scattering near $3a$ x $3a$ superstructure reflections indicate that local structural distortions related to the CDW/PLD state are likely to exist at temperature as high as room temperature [27-34]. We study the distortions by both conventional and resonant high-energy x-ray diffraction (XRD) coupled to atomic pair distribution function (PDF) analysis and reverse Monte Carlo (RMC) simulations in the temperature range from 400 K to 100 K, concentrating on the local arrangement of Ta atoms. Fine details of the arrangement are well revealed and thoroughly assessed to highlight the important role of local lattice distortions in the temperature-driven formation of the CDW/PLD state of 2H-$TaSe_2$.

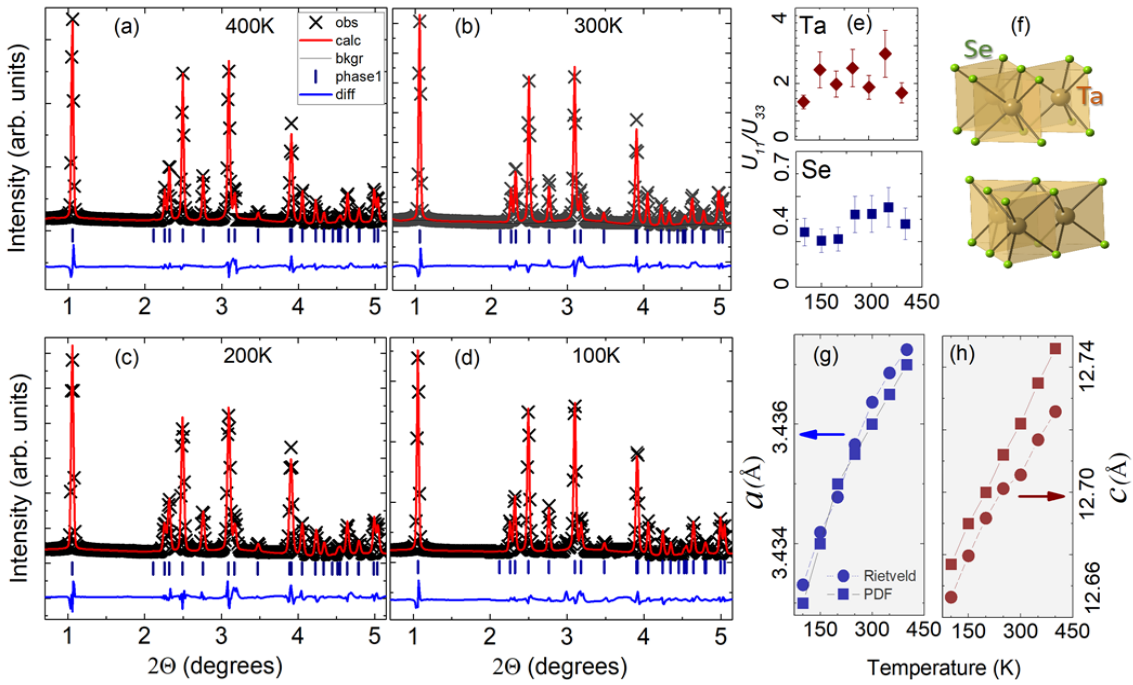

FIG. 1 (a) to (d) Rietveld fit (red line) to high-energy XRD patterns (symbols) for 2H-$TaSe_2$ collected at different temperature. The residual difference (blue line) is shifted by a constant factor for clarity. (e) Ratio of the anisotropic thermal factors u_{11} and u_{33} for Ta (red rhombuses) and Se (blue squares) atoms obtained by Rietveld analysis. (f) Fragment of the layers of Ta-Se trigonal prisms forming 2H-$TaSe_2$. (g) and (h) Hexagonal lattice parameters a and c for 2H-$TaSe_2$ as a function of temperature obtained by Rietveld (circles) and atomic PDF (squares) analysis.

High-quality 2H-$TaSe_2$ sample was provided by 2DSemiconductors [35]. It was subjected to XRD experiments using synchrotron x-rays with energy of 108.9 keV (λ=0.1173 Å) [36]. Exemplary XRD patterns collected at different temperature and results from Rietveld fits to the patterns are shown in FIG. 1(a-d). The fits confirm the hexagonal type (S.G. $P6_3/mmc$) of the average crystal structure of 2H-$TaSe_2$ and also show that its lattice parameters gradually diminish with decreasing temperature (FIG 1g, h). Refined thermal factors indicate that the amplitude of the in-plane rms vibrations of Ta atoms is twice that of the out-plane vibrations for all studied temperatures. The situation with the displacements of Se atoms is reversed (FIG. 1e). Thus, in line with the findings of prior studies [1, 20, 24], results of Rietveld analysis indicate the presence of significant positional disorder of Ta and Se atoms within and between the Ta-Se layers, respectively. Note that, due to their nature, XRD data reflect instantaneous positions of atoms and, hence, the observed disorder may reflect not only static but also possible dynamic rms atomic displacements.

Analysis of total atomic PDFs derived from high-energy XRD patterns provides more clues about the character of that disorder (FIG. 2). In particular, the atomic PDF for 2H-$TaSe_2$ obtained at 400 K may be well approximated with a model based on structure parameters, including lattice parameters, atomic positions and rms vibrational amplitudes, obtained by Rietveld analysis of the corresponding XRD pattern (FIG. 2b). The result indicates that, barring the large anisotropy of atomic vibrations, the local and average crystal structure of 2H-$TaSe_2$ are similar above room temperature. On the other hand, only the higher-r part of the atomic PDF for 2H-$TaSe_2$ obtained at 100 K, i.e. below T_{CDW}, may be well approximated by Rietveld fit derived structure parameters (FIG. 2c). The observation indicates significant divergence of the local structure of the CDW/PLD state of 2H-$TaSe_2$ from the average hexagonal crystal structure. Analysis of the low-r part of the PDFs indicates that structural features that may not be explained by the average crystal structure appear already at 300 K as a high- and low-r shoulder of the first and second PDF peak, respectively (FIG. 2d). The features become increasingly distinct with decreasing temperature, indicating that, upon cooling below room temperature, the near neighbor distances in 2H-$TaSe_2$ become multi-modal.

In particular, the first peak in the PDF for undistorted 2H-$TaSe_2$ would be well-defined, reflecting the set of identical distances between Ta atoms centering the perfect trigonal-prismatic units and Se atoms occupying the vertices of the units (Fig. 2a). The units appear increasingly distorted, i.e. different near neighbor Ta-Se distances emerge, as the CDW/PLD state of 2H-$TaSe_2$ is approached on cooling. Furthermore, the second peak in the PDF for undistorted 2H-$TaSe_2$ would also be well-defined, reflecting the equal in length Se-Se and Ta-Ta distances involving atoms from nearby perfect trigonal prismatic units (FIG. 2a). Unusually short either Ta-Ta or Se-Se distances emerge in 2H-$TaSe_2$ already near room temperature. The distances become more

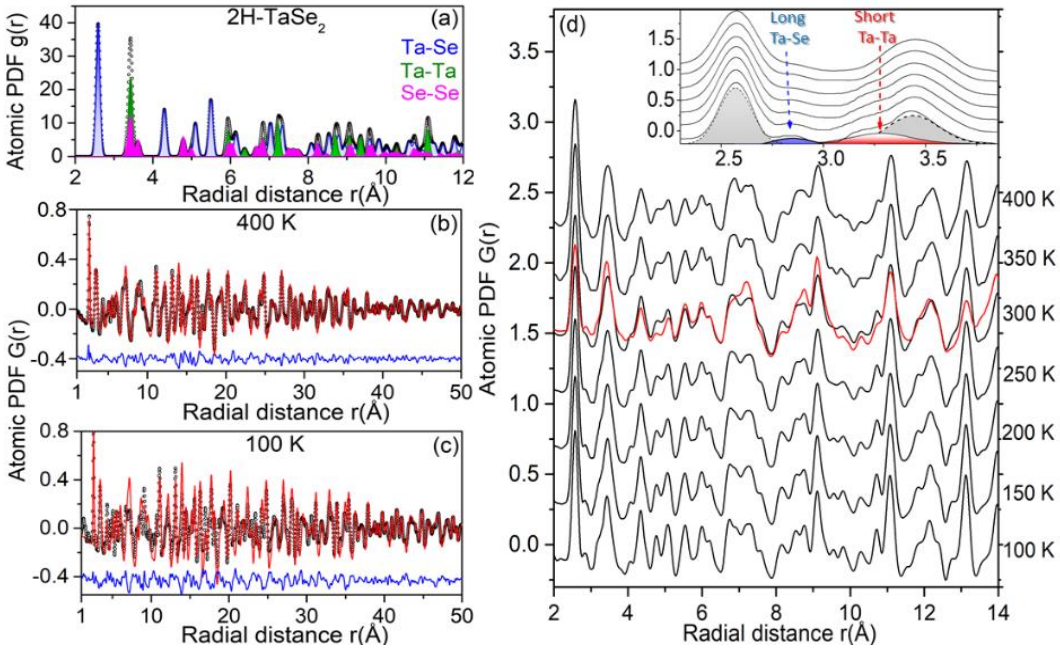

FIG. 2 (a) Computed total (symbols) and partial (colors) atomic PDFs for 2H-$TaSe_2$ showing the overlap of first neighbor Se-Se and Ta-Ta bonding distances in undistorted 2H-$TaSe_2$. (b) and (c) Fits (red line) to the experimental (symbols) total PDFs for 2H-$TaSe_2$ obtained at 400 K and 100 K. The residual difference (blue line) is shifted by a constant factor for clarity. The fits are based on a single unit cell model with a P6/3mmc symmetry. The low-r part of the 100 K PDF is poorly reproduced by the average hexagonal structure. (d) Low-r part of experimental total PDFs (black line) for 2H-$TaSe_2$ obtained at different temperature. Ta-differential PDF (red line) obtained by resonant high-energy XRD is also shown. The first two physical peaks of the total PDFs are shown in the inset. Arrows mark the evolution of peak shoulders reflecting the appearance of unusually long Ta-Se (blue) and short Ta-Ta (red) distances with decreasing temperature. Shaded areas emphasize long Ta-Se (blue), short Ta-Ta (red), and unmodified (black) Ta-Se and Ta-Ta bonding distances. Note that the observed misfit between the local and average structure in (c) and broad distribution of short Ta-Ta distances in (d) are reminiscent of the structural peculiarities exhibited by the CDW state of $CeTe_3$, where the PLDs involve the formation of an ordered pattern of distinct short and long Te-Te bonds [9].

distinct upon cooling, as indicated by the thermal evolution of the low-r shoulder of the second peak in the respective PDFs. To identify these distances, we conducted a resonant high-energy XRD experiment at the K edge of Ta. By its nature, the resulting Ta-differential atomic PDF reflects only structural features involving Ta atoms, that is, Ta-Se and Ta-Ta atomic pair correlations [36, 37]. In addition, it doubles the experimental sensitivity to the latter. For reference, the contribution of Ta-Ta atomic correlations to the total and Ta-differential PDFs for 2H-$TaSe_2$ is about 28 % and 50 %, respectively. Experimental Ta-differential PDF data help identify the low-r shoulder of the second PDF as unusually short Ta-Ta bonding distances (Fig. S3). Evidently, upon cooling below room temperature, some nearby Ta atoms in 2H-$TaSe_2$ come closer together in comparison to the average crystal structure.

To reveal the character of the apparent clustering of Ta atoms, we built large-scale 3D structure models using RMC [36]. The models were based on a 150 Å x 150 Å x 90 Å configuration of 80500 Ta and Se atoms cut out from the hexagonal lattice of 2H-$TaSe_2$. The large size of the model configuration allowed us to explore Ta-Ta pair correlations well beyond the 3*a* x 3*a* repetitive unit of the CDW/PLD state of 2H-$TaSe_2$. The configuration was refined against the total and Ta-differential PDF data obtained at 300 K and a model for the room temperature structure of 2H-$TaSe_2$ was produced. The model was used as an initial guess for the structure of 2H-$TaSe_2$ at 250 K and refined further against the respective PDF data. Following the same approach, we built a sequence of structure models tracking the evolution of local distortions of Ta planes in 2H-$TaSe_2$ upon cooling from above room temperature down towards T_{CDW}, where the first (I)-CDW/PLD phase is formed. The models reproduce the experimental PDF data in very good detail [FIG. S4].

Analysis of the RMC refined models shows that, above 300 K, Ta-Ta bonding distances in 2H-$TaSe_2$ exhibit a broad symmetric distribution centered at about 3.45 Å, i.e. that the rms displacements of Ta atoms are largely uncorrelated in nature. Clear signatures of correlated Ta displacements, appearing as unusually short Ta-Ta distances, emerge at 300 K. The distances become increasingly distinct with decreasing temperature, forming a pattern characteristic to the small-size clusters of Ta atoms known to exist in the CDW/PLD state of 2H-$TaSe_2$ (FIG. 3). The average value of the short distances is about 3.35(1) Å at 100 K [38]. Notably, not all clusters appear perfect at that temperature (FIG. 3f). However, when averaged out over the 3D model structure,

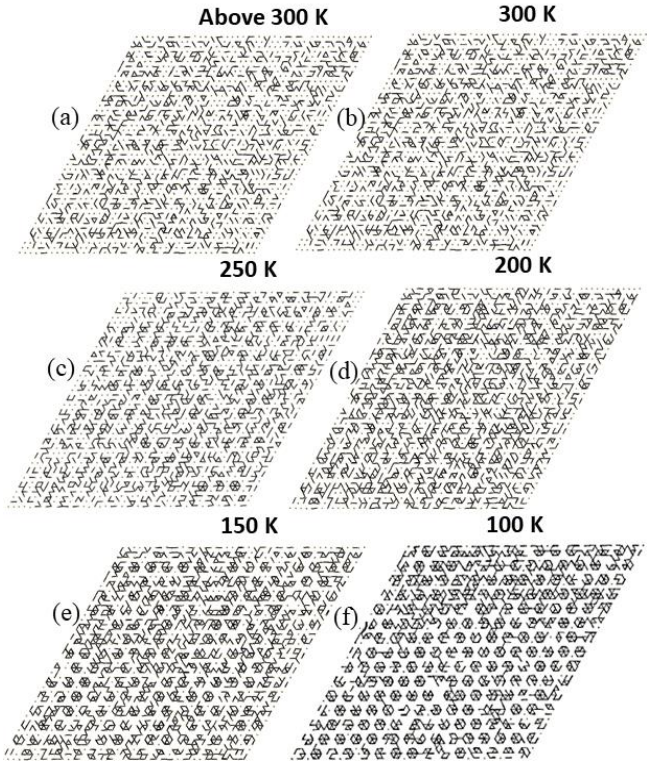

FIG. 3 Top view of 150 Å x 150 Å Ta planes in the 3D structure models for 2H-$TaSe_2$ representing the evolution of local lattice distortions with decreasing temperature. Dark short lines represent Ta-Ta bonding distances shorter than 3.40 Å. Such distances are present but are orientationally disordered at temperature above 300 K. The distances gradually become both more distinct and correlated with decreasing temperature, eventually forming a periodic pattern at 100 K, i.e. below T_{CDW}.

they appear consistent with the 3*a* x 3*a* superstructure of hexagons of 7 Ta atoms (FIG. 4a) suggested by prior experiments [20-27]. Likely because of the imperfections, the underlying crystal lattice appears somewhat distorted, i.e. not quite commensurate with the perfect hexagonal lattice of undistorted 2H-$TaSe_2$ (FIG. S7). Due to the in-plane clustering of Ta atoms and out-of-plane motion of Se atoms, Ta-Se units in the CDW/PLD state of 2H-$TaSe_2$ also appear distorted (FIG. S4) but, as analysis of Se-Ta-Se angles shows, their trigonal-prismatic geometry is largely preserved (Fig. S6).

The picture, which emerges for the formation of the superstructure of Ta atoms in the CDW/PLD state of 2H-$TaSe_2$, is therefore as follows (FIG. 3): Ta atoms suffer considerable in-plane positional disorder above room temperature, where thermal excitation effects appear to destroy possible correlations between their displacements. Short Ta-Ta bonds though do exist and are seen to become fairly correlated near room temperature. The correlations remain local with decreasing temperature, leading to the formation of small-size Ta clusters at about 200 K. The

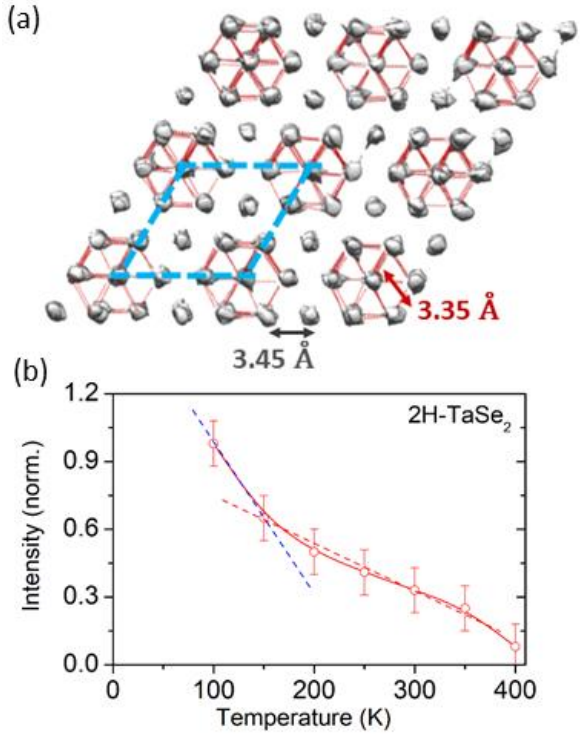

FIG. 4 (a) Top view of a "bulk-averaged" Ta plane in the first CDW/PLD phase of 2H-$TaSe_2$ obtained by mapping the respective 3D model onto a single Ta plane. The *3a* x *3a* superstructure unit cell of the phase is outlined with a blue line. Red broken lines highlight the presence of hexagon-shaped clusters of Ta atoms. The average distance between Ta atoms at the center and outer part of the clusters is 3.35(1) Å. The average distance between the latter and atoms that do not belong to the clusters is about 3.45(1) Å. Irregular gray spheres are contour plots of the "bulk-averaged" spatial (density) distribution of Ta atoms in the first CDW/PLD phase of 2H-$TaSe_2$, as evaluated from the respective 3D model. For clarity, the contour plots are terminated at density values smaller than 5 % of the maximum value. (b) Normalized intensity of the higher-r shoulder of the first peak in the PDF data as a function of temperature [see FIG. S8]. The intensity may serve as a "model-independent" parameter describing the temperature-driven evolution of local lattice distortions in 2H-$TaSe_2$ into the *3a x 3a* superstructure shown in (a). The evolution is seen to exhibit a kink close to T_{CDW}. The kink may be associated with the crossover between the pseudogap and band-gap regimes in 2H-$TaSe_2$ [32]. Also, it may be associated the observed kink in the transport properties of 2H-$TaSe_2$ [42].

clusters become distinct and clearly separated from each other at about 150 K. Likely, that is because they share peripheral atoms with their neighbors, and can no longer sustain a large distribution of Ta-Ta bond lengths/strength upon further cooling. Finally, at 100 K, i.e. below T_{CDW}, the clusters appear arranged in a distinct 3*a* x 3*a* periodic superstructure (FIG. 4a). Because the bonding distances between atoms in the clusters remain somewhat different, the clusters are unlikely to be completely aligned with each

other, thus leading to a finite average incommensurability of the emerged first CDW/PLD phase (FIG. S7). Upon further cooling the clusters are likely to become near perfect and lock into a commensurate superstructure to minimize the elastic energy [27, 33]. Upon a consequent warming/cycling in a narrow temperature range, the array of existing Ta clusters, or different parts of it, may follow a different spatial trajectory and even form multiple transient CDW/PLD phases, as observed by experiment [39-42].

In conclusion, experimental atomic PDF analysis and large-scale 3D structure simulations allow us to reveal the genesis of PLDs in the CDW phase of 2H-$TaSe_2$ in fine detail. We find that Ta atoms undergo significant in-plane rms displacements seen as unusually short Ta-Ta distances already near room temperature. The amplitude and direction of the displacements above T_{CDW} appear close to those of the static distortions of Ta planes observed below T_{CDW}. The differences is that the latter form a 3D periodic pattern whereas the former are correlated over short-range distances alone, with the correlation length gradually increases with decreasing temperature (FIG. 4b). Thus, the transition between the normal and CDW/PLD state of 2H-$TaSe_2$ appears gradual and, in this respect, the locally correlated displacements of Ta atoms above T_{CDW} may be looked at as a precursor of the PLDs below T_{CDW}. Such a relationship may well explain the emergence of a "precursor" CDW pseudogap in the normal state near room temperature and its smooth evolution into a band gap below T_{CDW} [32]. In particular, the pseudogap may be attributed to the locally correlated Ta displacements and the band gap may be understood as a consequence of the complete alignment of these displacements into a *3a* x *3a* superstructure. Our findings can also help improve our understanding of CDWs in low-dimensional solids beyond 2H-$TaSe_2$, including streamline theory relating the magnitude of PLDs, CDW energy gap and T_{CDW} [FIG. S9].

This work was supported by DOE-BES grant DE-SC0006877 and used resources of the Advanced Photon Source at the Argonne National Laboratory provided by the DOE Office of Science under contract no. DE-AC02-06CH11357. Thanks are due to Mr. O Shovon for the help with XRD experiments.

Corresponding author.
petko1vg@cmich.edu

[1] K. Rossnagel J. Phys.: Condens. Matter. **23**, 213001 (2011).
[2] X. Zhu, J. Guo, J. Zhang, and E. W. Plummer, Adv. Phys. **2**, 622 (2017).
[3] Chih-Wei Chen, J. Choe, and E. Morrosan, Rep. Prog. in Phys. **79**, 084505 (2016).
[4] U. Chatterjee, J. Zhao, M. Iavarone, R. Di Capua, J. P. Castella, G. Karappetkov, C. D. Mallakas, M. G. Kanatzidis, H. Claus, J. P. C. Ruff, F. Weber, J. van Wezel, J.C. Campuzano, R. Oswborn, M. Randeria, N. Trivedi, M. R. Norman, and S. Rozenkranz Nat. Commun. **6**:6313 (2015).
[5] L. Li, X. Deng, Z. Wang, Y. liu, M. Abeykoon, E. Dooryhee, A. Tomic, Y. Huang, J. B. Warren, E. S. Bozin, S. J. L. Billinge, Y. Sun, Y. Zhu, G. Kotliar, and C. Petrovic NPJ Quantum matter. **2**, 16 (2017).
[6] Y. Liu, D. F. Shao, L. J. Li, X. D. Zhu, P. Tong, R. C. Xiao, L. S. Ling, C. Y. Xi, L. Pi, H. F. Tian, H. X. Yang, J. Q. Li, W. H. Song, X. B. Zhu, and Y. P. Sun Phys. Rev. B **94**, 045131 (2016).
[7] K. Wijayaratne, J. Zhao, Ch. Malliakas, D. Y. Chung, M. G. Kanatzidis, and U. Chatterjee J. Mater. Chem. C **5**, 11310 (2017).
[8] S. van Smaalen Acta Cryst. A A61, 51 (2005).
[9] H. J. Kim, C. D. Malliakas, A. T. Tomic, S. H. Tessmer, M. G. Kanatzidis, and S. J. L. Billinge Phys. Rev. Lett. **96**, 226401 (2006).
[10] T. Egami and S. J. L. Billinge, *Underneath the Bragg Peaks: Structural Analysis of Complex Materials* (Pergamon, Oxford, England, 2003).
[11] V. Petkov, in *Characterization of Materials* (John Wiley & Sons, NY 2003).
[12] M. Kertesz and R. Hoffmann J. Am. Chem. Soc. **106**, 3453 (1984).
[13] C. Rovira and M.-H. Whangbo Inorg. Chem. **32**, 4094 (1993).
[14] A. Meetsma, G. A. Wiegers, R. J. Haange, and J. L. de Boer Acta Cryst. C**46**, 1598 (1990).
[15] H. Luo, W. Xie, J. Tao, H. Inoe, A. Gyenis, J. W. Krizan, A. Yazdani, Y. Zhu, and R. J. Cava PNAS **11**2, E1174 (2015).
[16] T. Ritschel, J. Trinckauf, K. Koepernik, B. Buchner, M. v. Zimmermann, H. Berger, Y. I. Joe, M. Abbamonte, and J. Geck, Nat. Phys. **11**, 328 (2015).
[17] M. Kratochvilova, A. D. Hiller, A. R. Wildes, L. Wang, S.-W. Cheong, and Je-G. Park NPJ. Quant. Mat. **2**, 42 (2017).
[18] D. Miller, S. D. Mahanti, and P. Duxbury Phys. Rev. B **97**, 045133 (2018).
[19] W. Wang, D. Dietzel, and A. Schirmeisen Sci. Rep. **9**:7006 (2019).
[20] D. E. Moncton, J. D. Ake, and F. J. DiSalvo, Phys. Rev. B **16**, 801 (1977).
[21] R. M. Fleming, D. E. Moncton, D. B. McWhan, and F. J. DiSalvo Phys. Rev. Lett. **45**, 576 (1980).
[22] T. Butz, S. Saibene, and A. Lerf, J. Phys. C: Solid State Phys. **19**, 2675 (1986).
[23] R. Brower and F. Jellinek Physica B+C **99**, 51 (1980).
[24] R. M. Fleming, D. E. Moncton, J. D. Axe, and G. S. Brown Phys. Rev. B **30**, 1877 (1984).
[25]. J. van Landuyt, G. van Tendeloo, and S. Amelinckx Phys. Stat. Sol. **A26**, 359 (1974).
[26] J. van Landuyt, G.A. Wiegers, and S. Amelinckx Phys. Stat. Sol. **A46**, 479 (1978).

[27] J. Dai, E. Calleja, J. Alldredge, X. Zhu, L. Li, W. Lu, Y. Sun, T. Wolf, H. Berger, and K. McElroy Phys. Rev. B **89**, 165140 (2014).
[28] D. S. Inosov, D. V. Evtushinsky, V. B. Zabolotnyy, A. A. Kordyuk, B. Bunchner, R. Follath, H. Berger, and S. V. Borisenko Phys. Rev. B **79**, 125112 (2009).
[29] R. L. Barnett, A. Polkovnikov, E. Demler, W.-G. Yin, and W. Ku Phys. Rev. Lett. **96**, 026406 (2006).
[30] S. Sugai, K. Murase, S. Uchida, and S. Tanaka J. de Physique **42,** C6-728 (1981).
[31] H. M. Hill, S. Chowdhury, J. R. Simpson, A. F. Rigosi, D. B. Newell, H. Berger, F. Tavazza, and A. R. H. Walker Phys. Rev. B **99**, 174110 (2019).
[32] S. V. Borisenko, A. A. Kordyuk, A. N. Yaresko, V. B. Zabolothyy, D. S. Isonov, R. Schuster, B. Buchenr, R. Weber, R. Follath, L. Patthey, and H. berger Phys. Rev. Lett. **100**, 196402 (2008).
[33] Ph. Leininger, D. Chernyshov, A. Bosak, H. Berger, and D. S. Inosov Phys. Rev. B **83**, 233101 (2011).
[34] W. Yim, W. ku, R. Barnett, and E. Demler Phys. Rev. Lett. **96**, 026406 (2006).
[35] http://www.hqgraphene.com/TaSe2.php
[36] See Supplemental Material at http://link.aps.org/ supplemental/……for supporting experimental and computational details.
[37] V.Petkov, S. Shastri, J.-Woo Kim, S. Shan, J. Luo, J. Wu and Ch.-J.Zhong Acta Cryst. A **74,** 553 (2018).
[38] Shrinking of Ta-Ta bonds in the order of 0.1 Å is reported by C. B. Scruby, in Ph.D. Thesis, p. 252 University of London (1976); https://spiral.imperial.ac.uk/handle/10044/1/22483.
[39] J. E. Inglesfield, Physica B+C **99**, 238 (1980).
[40] M. D. Johannes and I. I. Mazin Phys. Rev. B **77**, 165135 (2008).
[41] T.-Ru T. Han, F. Zhou, Ch. D. Malliakas, P. M. Duxbury, S. D. Mahanti, M. G. Kanatzidis, and Ch.-Yu Ruan Sci. Adv. 2015;1:e1400173 (2015).
[42] V. Vescoli, L. Degiorgi, H. Berger, and L. Forró, Phys. Rev. Lett. **81**, 453 (1998).